

Plain Abdominal Radiography: the gas pattern and the abdominal pathology

Radiografía simple de abdomen: una mirada a la patología abdominal a partir del patrón gaseoso

Felipe Aluja Jaramillo[1]
Ricardo Cuervo Arévalo[2]

https://doi.org/10.53903/01212095.201

Key words (MeSH)
Radiography, abdominal
Radiography
Intestinal obstruction
Abdominal pain

Palabras clave (DeCS)
Radiografía abdominal
Radiografía
Obstrucción intestinal
Dolor abdominal

Summary

Plain abdominal radiography is a tool available in almost any health institution. Medical professionals have difficulties in its interpretation which, in addition to its inherent limitations, casts doubt on the usefulness of this imaging method. Since its main emergency indication is abdominal pain with suspected intestinal obstruction, it is imperative to approach its analysis in an orderly manner, putting into practice previous knowledge of abdominal anatomy, technical requirements for adequate image acquisition, analysis of intra-abdominal gaseous pattern, solid organs, calcifications, foreign bodies and medical devices.

Resumen

La radiografía de abdomen simple es una herramienta disponible en casi cualquier institución de salud. Los profesionales médicos tienen dificultades en su interpretación, lo cual, además de sus limitaciones inherentes, pone en duda la utilidad de este método de imagen. Dado que su principal indicación de urgencia es el dolor abdominal con sospecha en obstrucción intestinal, es imperativo abordar su análisis de forma ordenada, poniendo en práctica los conocimientos previos de la anatomía abdominal, los requisitos técnicos para la adecuada adquisición de la imagen, el análisis del patrón gaseoso intraabdominal, los órganos sólidos, las calcificaciones, los cuerpos extraños y los dispositivos médicos.

Introduction

Abdominal radiography is one of the diagnostic modalities for the approach of abdominal pathologies, including, in some circumstances, thoracic pathologies (1, 2). However, after the advent of computed axial tomography (CT) it has lost relevance, since it has a lower diagnostic yield compared to other diagnostic modalities (3-5). Nevertheless, it is useful in the evaluation of some entities, especially in low complexity medical centers (6). This article aims to provide the necessary knowledge for a systematic approach to abdominal radiography, emphasizing the distribution of the intestinal gas pattern.

1. General Information

Indications

Abdominal radiography is useful in the patient with poorly localized abdominal pain, whether or not associated with other symptoms or clinical signs, and its main utility is the diagnosis of intestinal obstruction and its complications (7, 8). However, it is also useful to evaluate the position of medical devices and the search for foreign bodies (9).

Technique

An adequate abdominal radiography covers from the pulmonary bases to the pubic symphysis, both in its anteroposterior projection and in the standing position (10) (Figure 1). If the clinical condition of the patient warrants it, an anteroposterior projection should be performed with the patient in left lateral decubitus while the beam is incident horizontally to facilitate the visualization of the hydro-aerial levels or intra-abdominal free air (11) (figure 1). There are special posteroanterior projections in prone decubitus and anteroposterior in right lateral decubitus while the beam is irradiated horizontally, in order to evaluate the mechanical colonic ileus (11, 12).

Radiological anatomy

To understand the disease, the normal abdominal anatomy must be understood. The difference between the densities of the adjacent organs and fatty tissue makes it possible to identify the normal characteristics of the abdominal structures (13). Figure 2 represents the normal anatomy.

[1]Radiologist, specialist in Education for Health Professionals, Hospital Universitario San Ignacio, Pontificia Universidad Javeriana. Bogotá, Colombia.

[2]Radiology Resident, Pontificia Universidad Javeriana, Hospital Universitario San Ignacio. Bogotá, Colombia.

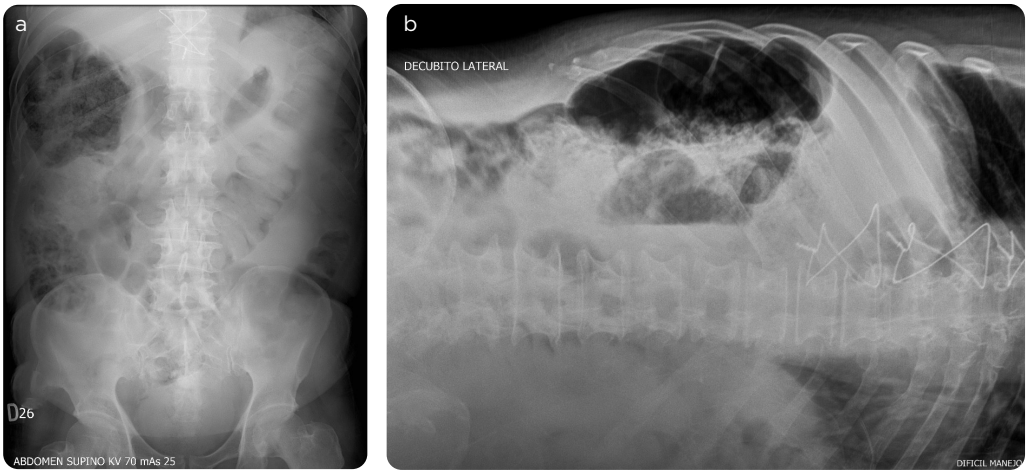


Figure 1. Projections in (a) standing and (b) left lateral decubitus with AP incident beam with perpendicular and horizontal beam, respectively, in an elderly patient, whose clinical condition made it difficult for her to sit up. The left lateral decubitus projection with horizontal beam allows the detection of extraluminal gas over the radiopaque silhouette of the liver.

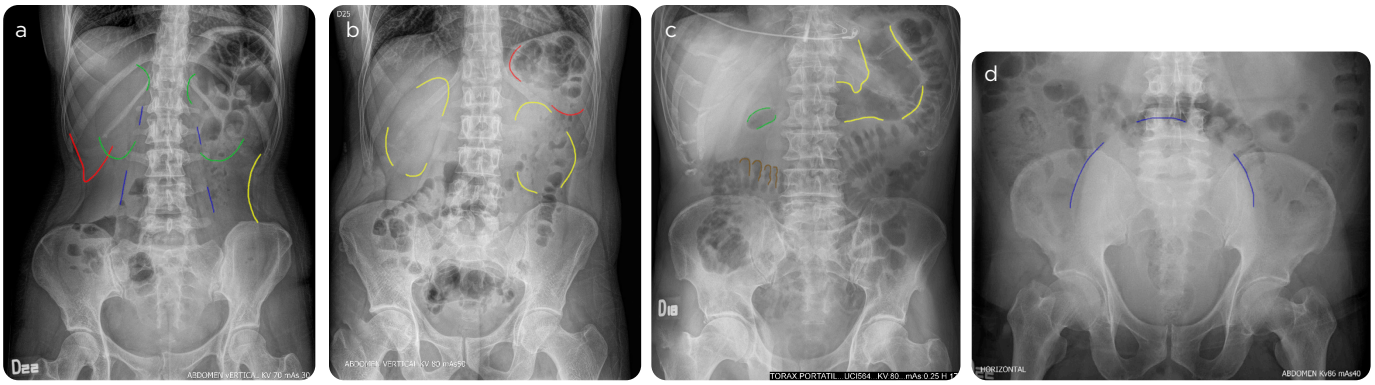


Figure 2. Normal anatomy. Supine abdominal radiographs. a) The red line delimits the lower hepatic contour, the green lines delimit the contours of both kidneys, the blue lines delimit the contours of both iliac psoas muscles and the yellow line delimits the lateroconal fascia. b) The yellow lines show the renal silhouettes, in red the splenic silhouette. c) The yellow lines delimit the gas within the gastric cavity, the green line the gas within the duodenum, and the red-wine line the gas of the transverse colon. d) The blue line delimits the bladder dome of a patient with acute urinary retention.

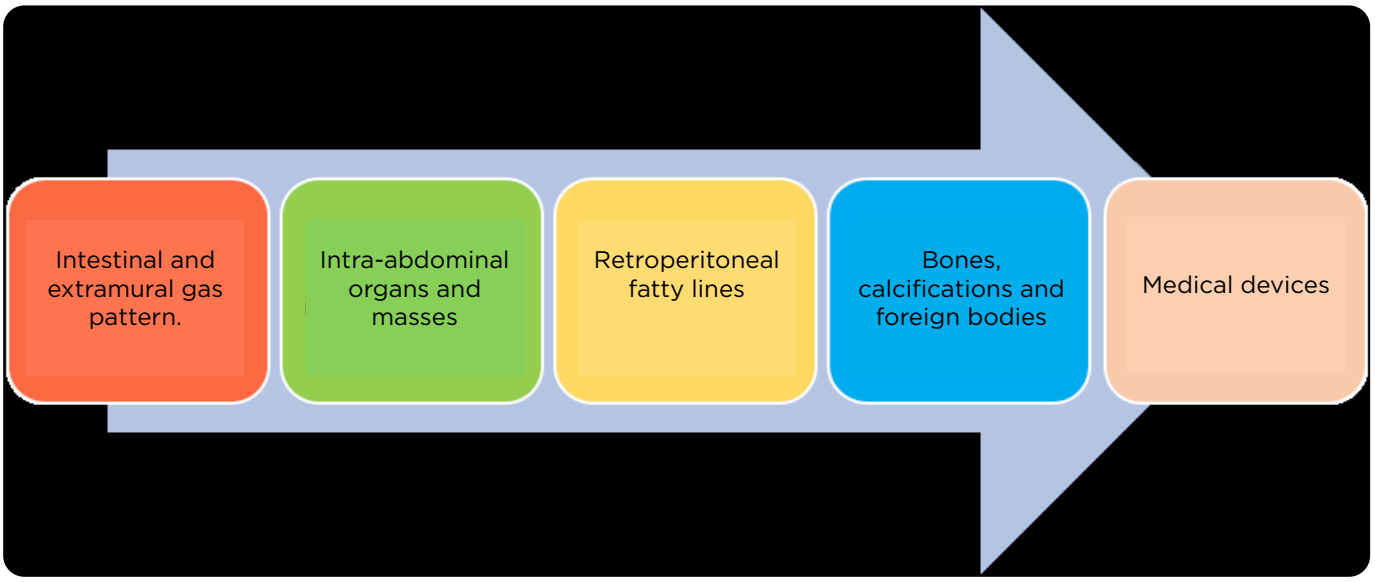


Figure 3. Proposed approach scheme.

Systematic evaluation

According to the approach proposed by Loo and collaborators (14), the analysis can begin with the identification of medical devices, followed by the evaluation of solid organs, retroperitoneal fatty lines or soft tissues of the abdominal wall, bones, calcifications or foreign bodies and, finally, the pattern of intra- and extraluminal intestinal gas (14). However, in our practice, the intestinal gas distribution pattern is of vital importance, which is why we recommend that it be the first item to evaluate (Figure 3).

2. Intestinal gas pattern

Normal distribution

It is considered normal to find gas in the gastric chamber, as well as in the first and second portions of the duodenum, colon and rectum. It is also normal to find up to two hydroaerial levels with a symmetrical arrangement in the same loop of the small intestine, in the transverse colon, sigmoid and rectum. In the colon, gas allows us to see the haustras as intraluminal indentations that do not cross the entire intestinal diameter. They are 1-4 mm thick and have a space of 1 cms between each one (12). Sometimes, the hepatic angle of the colon ascends to the inferior contour of the right hemidiaphragm, which is known as Chilaiditi's sign (15).

Abnormal distribution: how to interpret it

Occasionally, it is possible to demonstrate an abdominal radiograph without intestinal gas, a finding that is nonspecific, since it may be suggestive of benign or highly serious conditions. Among the causes of benignity is increased intestinal transit in episodes of viral gastroenteritis (16).

Generalized ileus

It is defined as the cessation of the normal propulsive peristalsis of the intestine, of non-mechanical cause, such as postoperative functional alteration, inflammation, neurological deficit of the mesenteric plexus, hydroelectrolytic or metabolic alterations (12-17, 18). It is evidenced as dilatation of the small bowel loops with a diameter greater than 3 cms, associated with at least two hydro-aerial levels with similar diameter in a U-shape, and concomitant dilatation of large loops greater than 6 cms (14-19,20). However, the cecum can present dilatation of up to 10 cms (14) (figure 4).

Focal ileus

It is defined as the alteration of normal propulsive peristalsis in a determined segment of the intestine, usually due to inflammatory or infectious processes of adjacent organs (21). The cardinal sign for its diagnosis is the sentinel loop, which is visualized as a set of one to three thin loops partially or totally distended in specific regions of the abdomen, for example, in the left hypochondrium, suggestive of acute pancreatitis (22).

Intestinal obstruction of small bowel loops

Intestinal obstruction is understood as the cessation of the transit of intestinal contents due to a mechanical cause, whether extrinsic, intrinsic or intraluminal. The most frequent cause is due to adhesions or postoperative flanges, included in the group of extrinsic etiologies (23). Unlike adynamic ileus, mechanical obstruction shows multiple thin loops with a dilatation greater than 2.5 cms in diameter, and more than two staggered hydroaerial levels, i.e. with a difference in height greater than 2 cms. In the standing projection a J-shaped pattern can be seen where the diameter of the hydroaerial levels is asymmetrical (23, 24) (Figure 5). In addition, it is usual to see little or no gas in the rectal or sigmoid ampulla, since in the absence of intestinal ischemia, the intestinal segment distal to the obstruction will remain with normal peristalsis until it evacuates all its contents in a normal mechanism to try to relieve the obstruction (12). However, in the case of very acute processes, it is still possible to visualize gas in the sigmoid and/or rectum. Another characteristic sign in standing projections is the "bead necklace", in which air bubbles are visualized between the connivent valves in an obstructed intestine full of liquid (25) (Figure 5A).

Intestinal obstruction of large bowel loops

The pathophysiological mechanism is similar to mechanical obstruction of the small bowel. Its most frequent cause is colon cancer (26). As the sigmoid is the narrowest and most redundant portion of the colon, it is the most susceptible to mechanical obstruction (26). Regarding the point of intestinal obstruction, the proximal loops dilate more than 6 cms, with the exception of the cecum whose starting point is 9 cms (27). Higher numbers increase the risk of rupture, associated with collapse of the distal colon and accumulation of gas and feces (27). It is usual to find pathological patterns of colonic gas in the form of volvulus or closed loop intestinal obstruction, in which an intestinal loop is obstructed at two different points using the mesentery as a pivot, increasing the risk of intestinal ischemia (12) (Figure 6).

The sigmoid colon is the most frequent site of occurrence of this phenomenon, probably because of its length and redundancy. It is more usual in older patients with chronic constipation and high fiber diet (12, 28, 29). In the images the classic signs are the "coffee bean sign" (figure 7) (30) and the "northern exposure sign", the latter characterized by the apex of the dilated sigmoid colon surpassing the transverse colon and pointing to the right hemidiaphragm, associated with the absence of rectal gas (31). As for the cecum or right colon, it is possible that it presents torsion as long as its union to the posterior parietal peritoneum is incomplete (12). The excess of mobility allows the displacement of the caecum volvulus to other regions of the abdomen, frequently the mesogastrium or the left hypochondrium. In the images a blind, distended loop of colon will be observed, with an indentation in its medial contour (representing the ileocecal valve), with staggered hydroaerial levels (12). This type of volvulus is rare; however, it is part of the range of differential entities of mechanical obstruction of the large bowel.

3. Gases in other locations

Air in the intestinal wall

Intestinal pneumatosis is the accumulation of gas between the walls of the intestine. It usually occurs due to iatrogenic causes, ischemia, chronic obstructive pulmonary disease, chemotherapy, collagen-vascular diseases, scleroderma, Whipple's disease, among others (32). In the abdominal radiography, round or linear radiolucent images can be observed in the form of small bubbles between the thickness of the intestinal wall (12, 14, 33, 34).



Figure 4. Abdominal X-ray in the supine position. There is evidence of marked dilatation of the small and large intestinal loops, with gas in the rectal ampulla and material of heterogeneous density in the colic frame. The image corresponds to an older adult patient with chronic constipation who consults for abdominal distension and absence of bowel movements for more than 20 days.

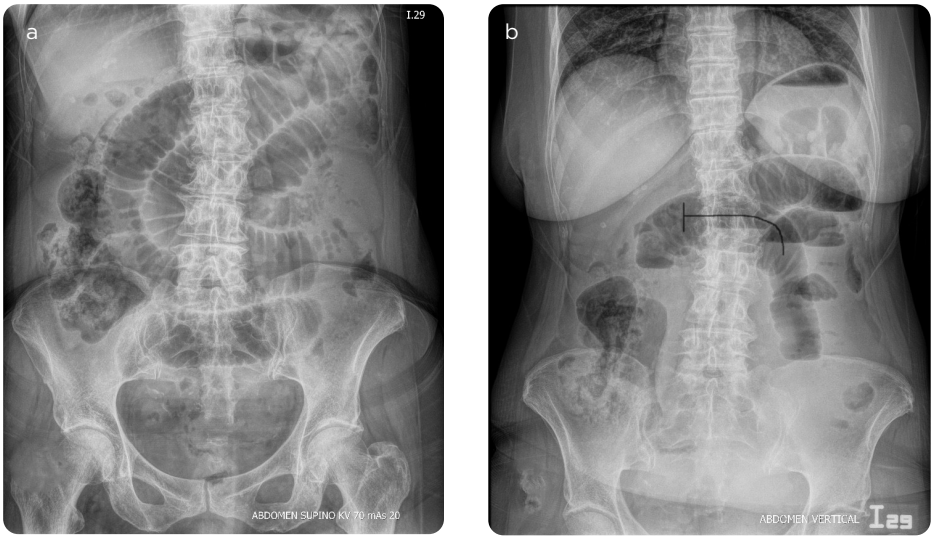


Figure 5. a) Supine abdominal radiograph. There is a pattern of intestinal obstruction with several thin intestinal loops with a dilation greater than 3 cms in diameter. b) Standing projection. Several hydroaereal levels are observed in which a central loop shows two staggered hydroaereal levels of asymmetric diameter, configuring a J-shaped pattern suggestive of mechanical obstruction.

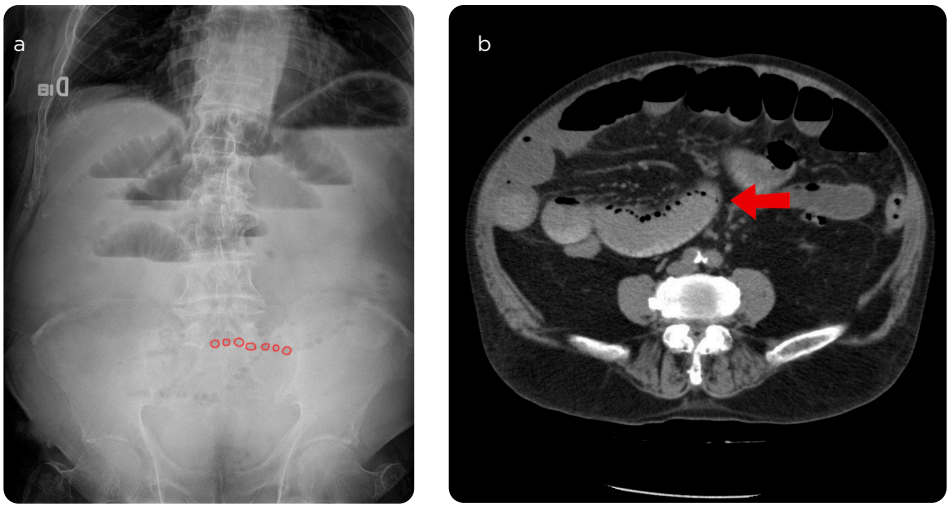


Figure 6. a). X-ray of the abdomen in standing position. Several dilated thin intestinal loops are shown with several staggered hydro-aerial levels configuring an obstructive pattern. Delimited by red circles, several consecutive small oval radiolucent radiolucent images are observed, forming the "bead necklace" sign. b). Abdominal CT with contrast medium of the same patient. The red arrow points to several endoluminal hypodense images in a dilated small bowel loop, corresponding to gas between the connivent valves, similar to the "bead necklace" sign in the abdominal radiography.

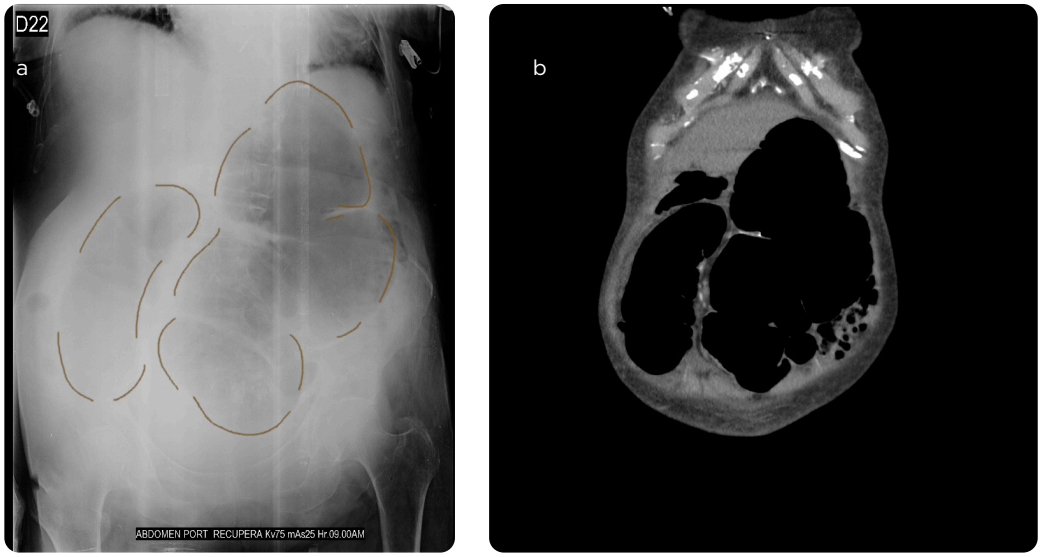


Figure 7. a) Abdominal X-ray in supine position: marked dilatation of large intestinal loops configuring the sign delimited by brown lines. b) Imaging representation of the sign in an abdominal CT in the same patient who presented a volvulus of the colonic cecum with the need of hemicolectomy and ileocolonic anastomosis.

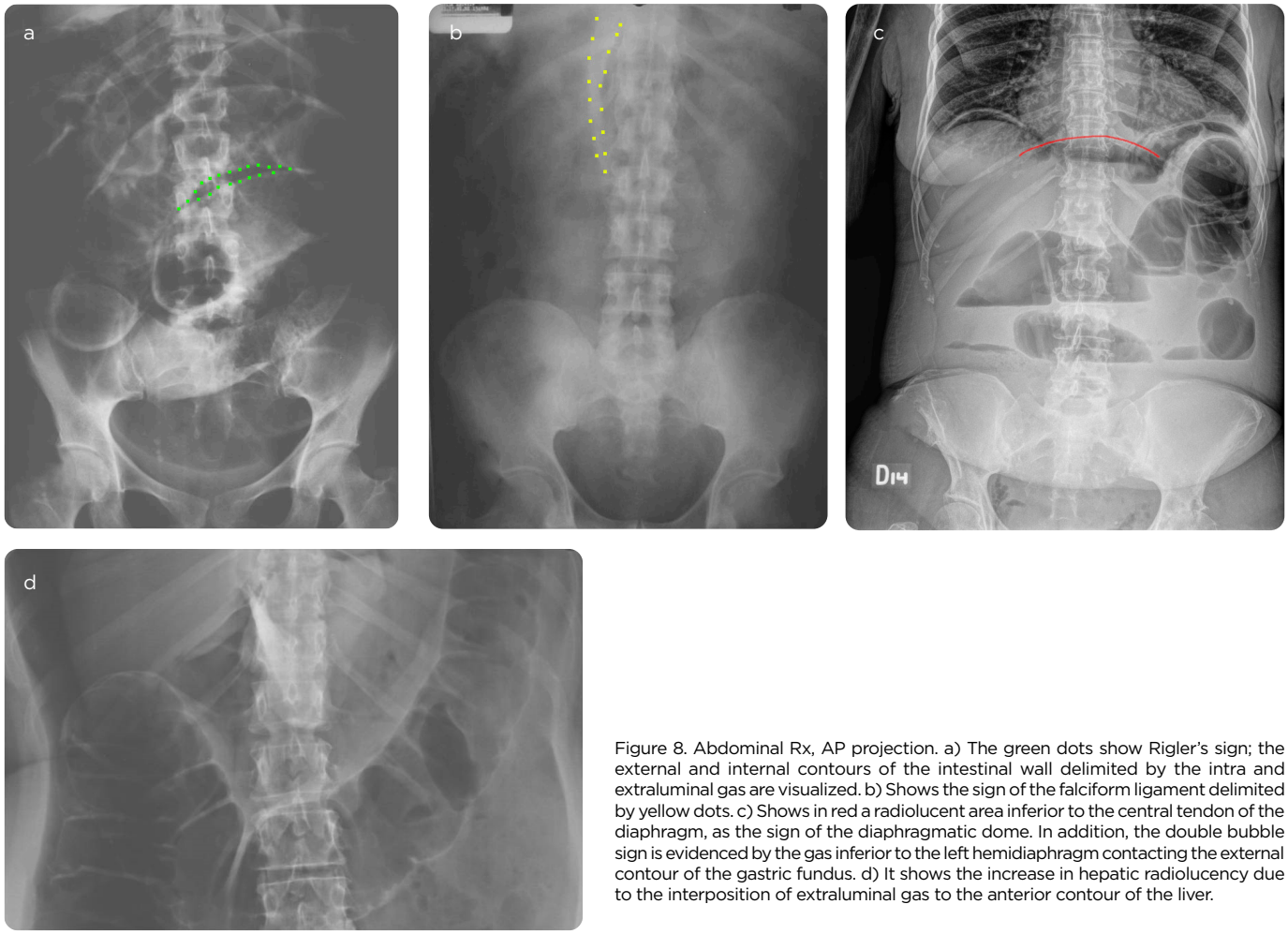


Figure 8. Abdominal Rx, AP projection. a) The green dots show Rigler's sign; the external and internal contours of the intestinal wall delimited by the intra and extraluminal gas are visualized. b) Shows the sign of the falciform ligament delimited by yellow dots. c) Shows in red a radiolucent area inferior to the central tendon of the diaphragm, as the sign of the diaphragmatic dome. In addition, the double bubble sign is evidenced by the gas inferior to the left hemidiaphragm contacting the external contour of the gastric fundus. d) It shows the increase in hepatic radiolucency due to the interposition of extraluminal gas to the anterior contour of the liver.

Extraluminal gas

Extraluminal gas is any gas that is not found in the lumen of the intestinal loops. It includes pneumoperitoneum, portal gas, pneumobilia, pneumoretroperitoneum and intestinal pneumatosis, among others.

Pneumoperitoneum

It is the accumulation of gas in the peritoneal cavity after perforation of a hollow intraperitoneal viscera or in postoperative states (12). The following are the most common signs:

- Rigler's sign: both the outer and inner walls of an intestinal loop are visualized by extraluminal gas adjacent the outer intestinal walls. It can be seen as a radiolucent triangle between the intestinal loops (35) (figure 8a).
- Sign of the falciform ligament: it is the visualization of a radio-opaque line that starts from the liver in the direction of the midline, usually showing the normal trajectory of the falciform ligament (36) (figure 8b).
- Dome sign: the air below the central tendon of the diaphragm shows the shape of a dome similar to architectural buildings (37) (figure 8c).
- Double bubble sign: the intraperitoneal subdiaphragmatic gas is seen aligned with the gas of the gastric fundus (14) (figure 8c).
- Hepatic radiolucency sign: it is the geographic lucidity on the hepatic silhouette or in the intraperitoneal subhepatic space, where the gas is found between the posterior wall of the right hepatic lobe and the anterior face of the right kidney, forming a triangular figure (38) (figure 8d).
- Radiolucency sign of the gastric lesser curvature: indicates gas in the transcavity of the omentum (14).

Portal venous gas and pneumobilia

It is the presence of gas in the portal venous system due to multiple causes (39, 40): from necrotizing enterocolitis or intestinal ischemia to benign causes such as gas of iatrogenic origin after intestinal surgery or endoscopic retrograde cholangiopancreatography (ERCP). In radiography it is identified as radiolucent serpentiform lines on the topography of the liver, branching as they extend towards the periphery. Its main differential diagnosis is pneumobilia, identified as radiolucent reticular lines projected on the central hepatic topography (40). Additionally, seeing them in an adult patient with intestinal obstruction suggests the presence of a biliary ileus, characterized by Rigler's triad: pneumobilia, intestinal obstruction and radiolucent calculus in the intestine (41) (figure 9).

Pneumoretroperitoneum

The location of the retroperitoneal gas guides us to the possible organ involved; for example, finding retroperitoneal gas projected in the right hypochondrium is indicative of rupture of the duodenum, with extraluminalization of gas in the right pararenal space. However, the location of the gas is not exclusive to the organ that occupies that place, since the rupture of the rectum can release retroperitoneal gas towards the anterior, posterior or perirenal pararenal spaces (42).

4. Beyond the gas pattern: Intra-abdominal organs and masses, what can be evaluated?

Fatty lines in solid organs are formed by the change in X-ray beam attenuation between adjacent fat/water and organ parenchyma, allowing some intra-abdominal organs to be identified and evaluated. However, observing fatty lines that form structures of variable size, in unusual locations and that displace intra-abdominal organs suggest solid, cystic or mixed space-occupying masses in the abdominal cavity, of congenital, infectious, inflammatory, traumatic, reactive or neoplastic origin of solid organs, hollow viscera or peritoneum (43) (Figure 10).

Liver

In cases of hepatomegaly the contours of the liver silhouette should exceed the superior border of the right iliac crest, the lateral border of the right psoas, displace the right renal contour, the duodenal bubble below the L2 vertebra, or elevate the right hemidiaphragm (44, 45) (Figure 11).

Spleen

Splenomegaly may be suspected with elevation of the left hemidiaphragm, displacement of the gastric bubble toward the midline, and descent of the splenic angle more caudal to the last rib (12, 46).

Kidneys

In addition to evaluating the size and location, it is possible to evaluate abnormalities in their contours, providing diagnostic suspicion of renal cystic disease or tumors (12).

Intestinal loops

The absence of intraluminal gas is not only indicative of proximal intestinal obstruction; sometimes it represents thickening of the intestinal wall due to inflammatory or neoplastic processes that displace gas, such as colon carcinoma, which assumes a density similar to that of an intra-abdominal solid organ and displaces adjacent structures (Figure 12).

5. Intra-abdominal fluid: to see or suspect it

In cases of intra-abdominal free fluid or ascites, an increase in the generalized radio-opacity of the abdomen can be observed with centralization of the intestinal loops, moving away from the fat lines, and the absence of the intraperitoneal fat lines and visceral lines (12, 47) (Figures 13 and 14).

There are some direct signs of ascites, such as obliteration of the hepatic margin, increase of the distance of the right properitoneal line with the ascending colon of more than 2-3 mm or Hellmer's sign, where the lower hepatic tip is displaced towards the lateral wall of the abdomen (48, 49).

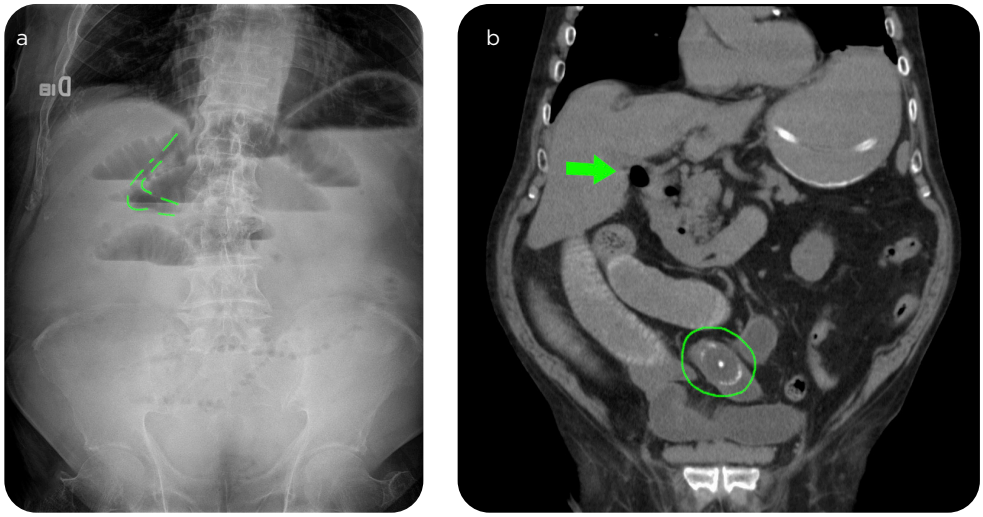


Figure 9. Elderly patient who consulted for abdominal pain, emesis and jaundice, who subsequently developed a mechanical obstruction of the small intestine by an enterobiliary fistula configuring a biliary ileus. a) Plain abdominal radiograph in standing position. The "bead necklace" sign is observed in the presence of a mechanical obstruction of small intestinal loops. Delimited by green lines there are radiolucent areas that project near the hilum of the hepatic silhouette, the most cephalic shows air in the left intrahepatic bile duct, the most caudal the common hepatic duct. b) CT of the abdomen with contrast medium: the green arrow points to a low density area corresponding to an air bubble in the biliary tract; surrounded by a green circle an oval image, with high density contours, corresponding to a gallstone, as the cause of the obstruction.

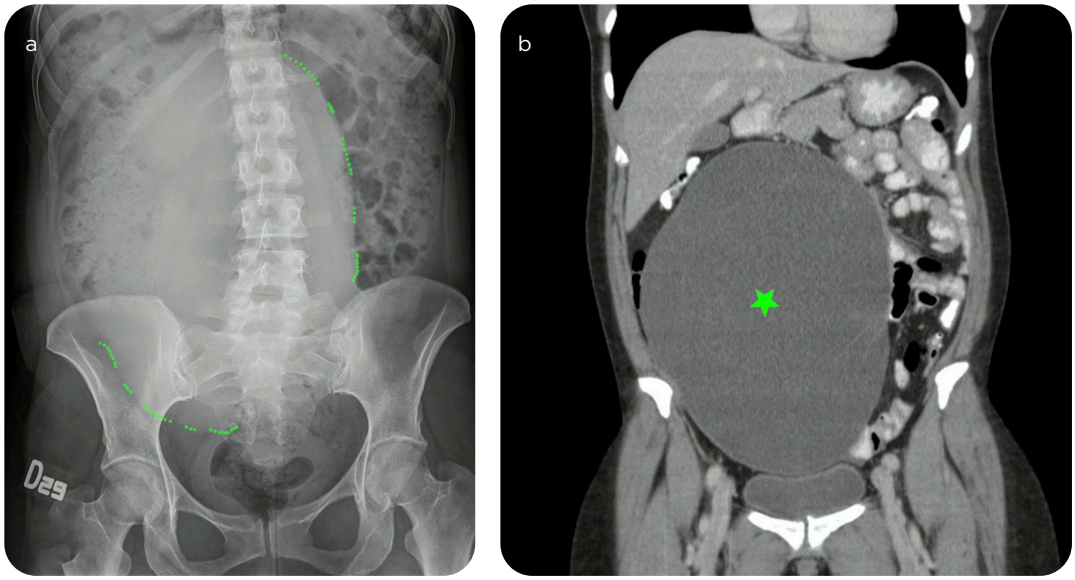


Figure 10. a) Supine abdominal radiograph showing a radio-opaque structure occupying space in the mesogastrium and greater pelvic cavity with successive green dots, which displaces the small and large intestinal loops in an eccentric manner. The intraluminal bowel gas pattern is normal. The retroperitoneal fatty lines are preserved. b) CT of the abdomen with oral and intravenous contrast medium, coronal reconstruction of the same patient, showing (green star) an oval, well-delimited, hypodense, thin-walled lesion with some internal septa that enhance with intravenous contrast medium.

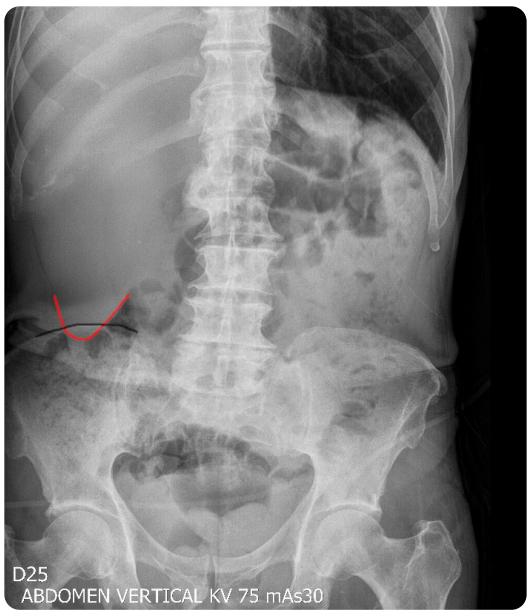


Figure 11. Plain abdominal radiograph in the standing position: the lower hepatic contour exceeding the upper contour of the right iliac crest (black line) in a patient with hepatomegaly is demarcated with red.

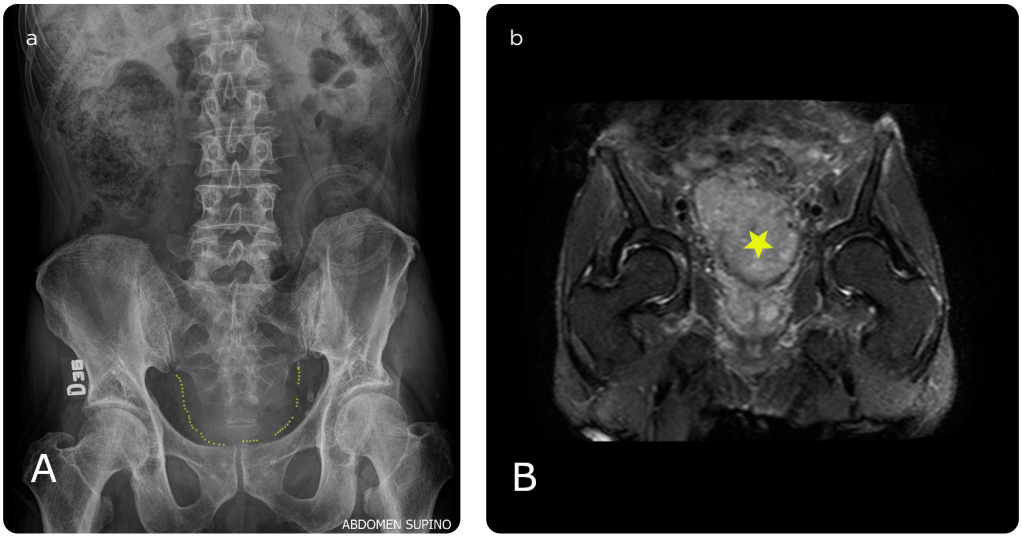


Figure 12. a) Simple abdominal radiograph in supine position in which, by means of successive yellow dots, a radiopaque mass with density similar to the intra-abdominal solid organs is delimited, located in the topography of the sigmoid colon and rectum. Note the absence of intraluminal gas usual in this location. b) MRI of the same patient, coronal T1-weighted slice with fat suppression STIR: a well-defined high signal mass with lobulated contours replacing the rectal cavity is marked with a yellow star. The findings represent a carcinoma of the rectum.

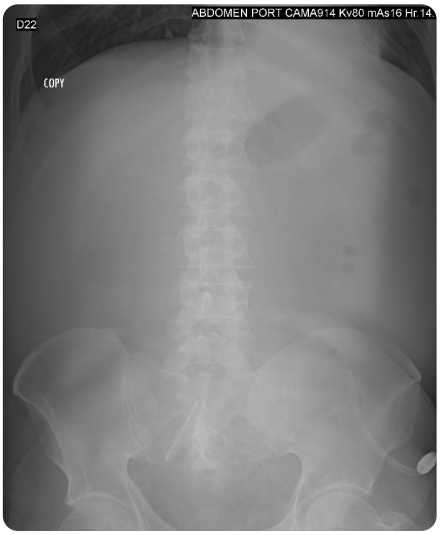


Figure 13. Plain abdominal radiograph: absence or effacement of intraperitoneal fatty lines delineating the contours of the psoas muscle and intraperitoneal solid organs in a patient with chronic kidney disease on peritoneal dialysis. The peritoneal drainage catheter can be seen in the left iliac fossa.



Figure 14. Abdominal X-ray: effacement of the intra- and retroperitoneal fatty lines with centralization of the intestinal gas pattern of the colon and small bowel portions is observed. Findings suggestive of ascites in a patient with stage IV metastatic breast cancer, with peritoneal progression, with malignant ascites.

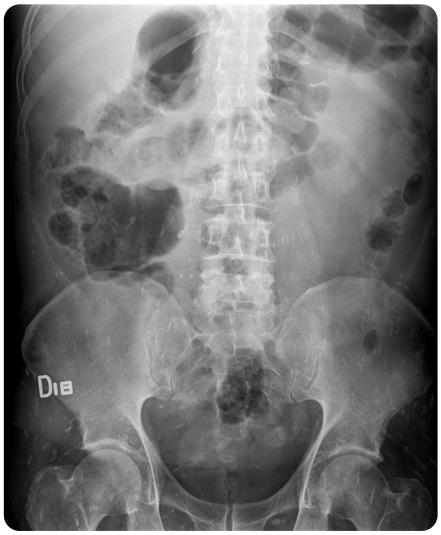


Figure 15. Simple abdominal radiograph in the supine position: multiple small, tubular, radio-opaque images with a "grain of rice" morphology distributed diffusely in the abdomen. They are more evidently observed in the topography of the iliac ailerons and the iliac psoas muscles. Image compatible with cutaneous and muscular cysticercosis in a patient who consulted for gastrointestinal who consulted for gastrointestinal symptoms.

6. Radio-opaque images and calcifications: what do they represent?

Calcifications are the accumulation of calcium crystals in diseased or healthy tissues through the process of dystrophic and metastatic calcification, respectively (12, 50, 51). Their morphology and distribution in the abdomen provide information of their organ of origin or possible underlying pathologic process, including both soft tissues and the skeleton of the abdominal region.

The calculi (biliary or renal) can be round or oval, with smooth, well-defined contours and their center is usually radio-opaque, with variable sizes (12, 52).

When their origin is biliary they are usually projected on the right hypochondrium while when their origin is renal they can be projected on the renal silhouettes. Regarding the visualization of gallstones, these can range from lamellar to multifaceted calcifications in the topography of the gallbladder or biliary tract (53). Calcified myomas usually present a similar pattern of mineralization; however, their location in the female pelvis, number and oval or round morphology suggest the diagnosis (12, 50).

Irregular, small, diffuse, diffuse and projected calcifications in the epigastrium can be seen in cases of chronic pancreatitis (54). However, identifying them in a random distribution pattern, without topographic predilection of any abdominal organ and elongated or "rice grain" morphology, suggests parasitic infectious processes such as cysticercosis (12, 50) (Figure 15).

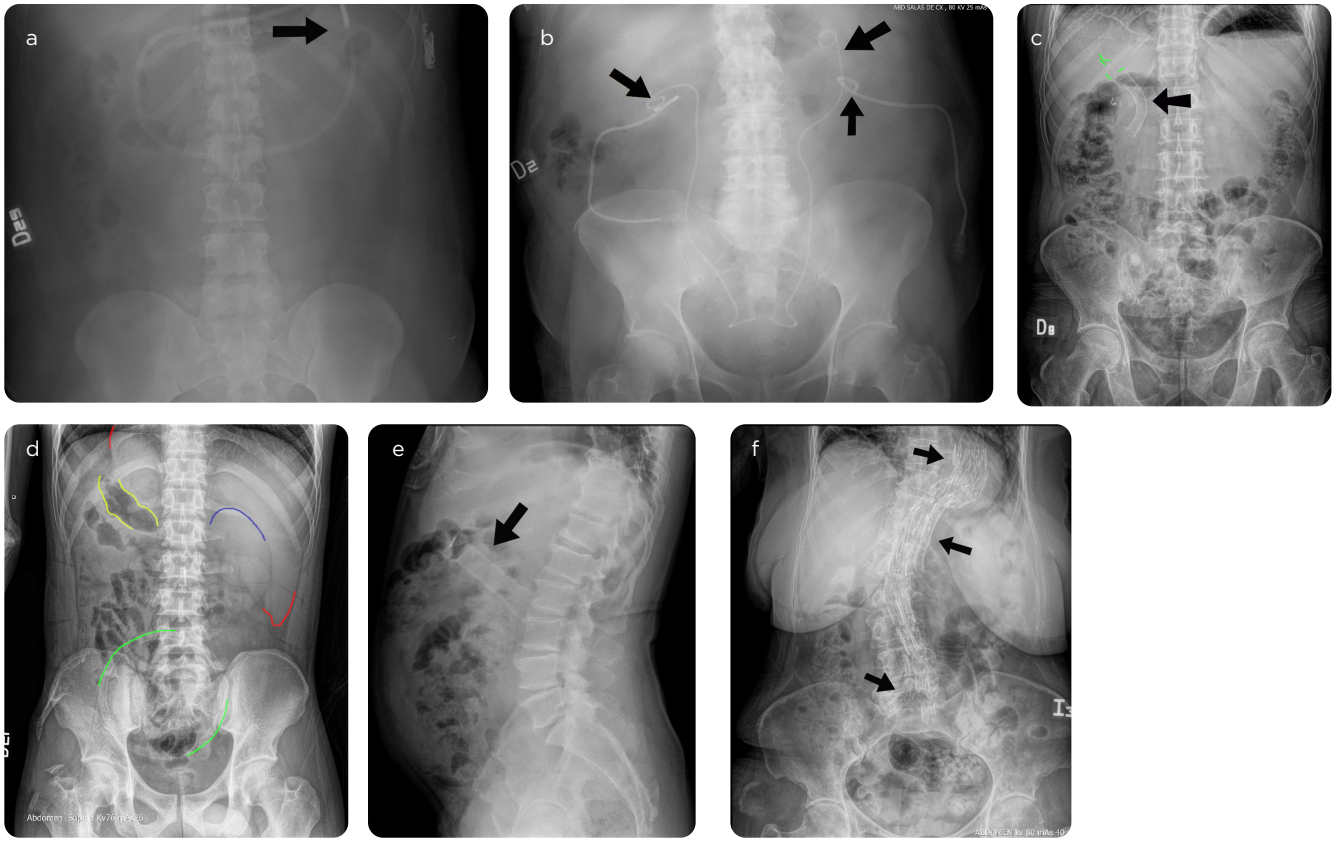


Figure 16. Abdominal radiographs. a) Advanced nasogastric tube with distal end in the third portion of the duodenum (black arrow), properly positioned. b) Four linear radio-opaque images whose coiled ends are projected over the topography of the renal pelvis and the ureteral tracts on both sides (black arrows) attributable to two nephrostomy catheters and two double J catheters. c) A metallic stent (black arrow) with adjacent radiolucent reticular images highlighted in green corresponding to pneumobilia, in the context of a biliary tract stent, is observed on the topography of the hepatic hilum. d) In a green circle an ostomy pouch frame in a patient with an entero-environmental fistula, additionally, in red color, the infrequent location of the liver and the cardiac apex in opposite location in a reverse situs, as well as the gastric chamber in blue and the descended left kidney. e) Esophageal stent that has migrated to the duodenal region (black arrow) in a patient with adenocarcinoma of the gastroesophageal junction. f). Radiography: extensive thoracic and abdominal aortic prosthesis (black arrows) in a patient with successful exclusion of thoracoabdominal aneurysm with covered stent placement.

7. Medical devices and foreign bodies

Naso-orogastric, enteral nutrition and ventriculoperitoneal shunts are observed as radio-opaque lines within the gastrointestinal lumen or intraperitoneal trajectory. Naso-orogastric tubes show their distal end in the gastric fundus or body; on the other hand, enteral or jejunal tubes should show their distal end beyond the third duodenal portion (55, 56). It is of vital importance to describe the location of its distal end in order to define new interventions or repositioning. There are other medical devices that can be frequently seen in the abdominal radiograph, such as suture clips, stents, multipurpose catheters or intrauterine devices (Figure 16) (55, 56).

Conclusion

Abdominal radiography continues to be a useful tool in medical practice settings. Despite the existence of other diagnostic modalities, it continues to be widely used as an initial method because of its availability and low cost; it is especially important for suspected intestinal obstruction or perforation, foreign body ingestion and location of medical devices. It is essential to reinforce and remember the systematic approach to this imaging modality, as it is often the first step in the comprehensive evaluation of the patient.

References

1. Eastman Kodak Company staff. Elementos de radiografía. Eastman Kodak; 1980.
2. Scheirey C, Fowler C, Therrien J, Kim D, Al-Refaie W, CamachoM, et al. ACR appropriateness criteria® 1 acute nonlocalized abdominal pain American college of radiology [Internet]. S. f. [citado: 2022 ene 27]. Disponible en: https://acsearch.acr.org/docs/69467/Narrative/
3. Ahn SH, Mayo-Smith WW, Murphy BL, Reinert SE, Cronan JJ. Acute nontraumatic abdominal pain in adult patients: abdominal radiography compared with CT evaluation. Radiology. 2002;225(1):159-64. http://dx.doi.org/10.1148/radiol.2251011282
4. Pandharipande PV, Reisner AT, Binder WD, Zaheer A, Gunn ML, Linnau KF, et al. CT in the emergency department: A real-time study of changes in physician decision making. Radiology. 2016;278(3):812-21. http://dx.doi.org/10.1148/radiol.2015150473
5. MacKersie AB, Lane MJ, Gerhardt RT, Claypool HA, Keenan S, Katz DS & Tucker JE. Nontraumatic acute abdominal pain: unenhanced helical CT compared with three-view acute abdominal series. Radiology. 2005;237(1):114-22. https://doi.org/10.1148/radiol.2371040066.
6. Eisenberg RL, Heineken P, Hedgcock MW, Federle M, Goldberg HI. Evaluation of plain abdominal radiographs in the diagnosis of abdominal pain. Ann Surg. 1983;197(4):464-9. http://dx.doi.org/10.1097/00000658-198304000-00016
7. Aras MH, Miloglu O, Barutcugil C, Kantarci M, Ozcan E, Harorli A. Comparison of the sensitivity for detecting foreign bodies among conventional plain radiography, computed tomography and ultrasonography. Dentomaxillofac Radiol. 2010;39(2):72-8. http://dx.doi.org/10.1259/dmfr/68589458
8. Hunter TB, Taljanovic MS. Medical devices of the abdomen and pelvis. Radiographics. 2005;25(2):503-23. http://dx.doi.org/10.1148/rg.252045157

9. Coursey CA, Casalino DD, Remer EM, Arellano RS, Bishoff JT, Dighe M, et al. ACR appropriateness criteria® acute onset flank pain–suspicion of stone disease. Ultrasound Q. 2012;28(3):227-33. http://dx.doi.org/10.1097/ruq.0b013e3182625974
10. Bontrager KL, Lampignano J. Textbook of radiographic positioning and related anatomy. 8a ed. Londres, Inglaterra: Mosby; 2014.
11. Laufer I. The left lateral view in the plain-film assessment of abdominal distension. Radiology. 1976;119(2):265-9. http://dx.doi.org/10.1148/119.2.265
12. Gore RM, Levine MS. Textobook of gastrointestinal radiology Vol 2. Elsevier; 2015.
13. Whalen JP, Berne AS, Riemenschneider PA. The extraperitoneal perivisceral fat pad. I. Its role in the roentgenologic visualization of abdominal organs: I. Its role in the roentgenologic visualization of abdominal organs. Radiology. 1969;92(3):466-72. http://dx.doi.org/10.1148/92.3.466
14. Loo JT, Duddalwar V, Chen FK, Tejura T, Lekht I, Gulati M. Abdominal radiograph pearls and pitfalls for the emergency department radiologist: a pictorial review. Abdom Radiol (NY). 2017;42(4):987-1019. http://dx.doi.org/10.1007/s00261-016-0859-8
15. Nair N, Takieddine Z, Tariq H. Colonic interposition between the liver and right diaphragm: The "Chilaiditi sign". Can J Gastroenterol Hepatol. v.2016;2016. PMC4904707.
16. Thompson WM. Gasless abdomen in the adult: What does it mean? AJR Am J Roentgenol. 2008;191(4):1093-9. http://dx.doi.org/10.2214/ajr.07.3837
17. Seaman WB. Motor dysfunction of the gastro-intestinal tract. Am J Roentgenol Rad Ther Nucl Med. 1972;116(2):235-44.
18. Böhm B, Milsom JW, Fazio VW. Postoperative intestinal motility following conventional and laparoscopic intestinal surgery. Arch Surg. 1995;130(4):415-9. http://dx.doi.org/10.1001/archsurg.1995.01430040077017
19. Kammen BF, Levine MS, Rubesin SE, Laufer I. Adynamic ileus after caesarean section mimicking intestinal obstruction: findings on abdominal radiographs. Br J Radiol. 2000;73(873):951-5. http://dx.doi.org/10.1259/bjr.73.873.11064647
20. Musson RE, Bickle I, Vijay RKP. Gas patterns on plain abdominal radiographs: a pictorial review. Postgrad Med J. 2011;87(1026):274-87. http://dx.doi.org/10.1136/pgmj.2009.082396
21. Ali N, Leshchinskiy S, Johnson M, D'Agostino R. The sentinel loop sign. Abdom Radiol (NY). 2018;43(11):3192-4. http://dx.doi.org/10.1007/s00261-018-1582-4
22. Davis S, Parbhoo SP, Gibson MJ. The plain abdominal radiograph in acute pancreatitis. Clin Radiol. 1980;31(1):87-93. http://dx.doi.org/10.1016/s0009-9260(80)80088-2
23. Silva AC, Pimenta M, Guimarães LS. Small bowel obstruction: what to look for. Radiographics. 2009;29(2):423-39. http://dx.doi.org/10.1148/rg.292085514
24. Harlow CL, Stears RL, Zeligman BE, Archer PG. Diagnosis of bowel obstruction on plain abdominal radiographs: significance of air-fluid levels at different heights in the same loop of bowel. AJR Am J Roentgenol. 1993;161(2):291-5. http://dx.doi.org/10.2214/ajr.161.2.8333364
25. Burgess LK, Lee JT, DiSantis DJ. The String of pearls sign. Abdom Radiol (NY). 2016;41(7):1435-6. http://dx.doi.org/10.1007/s00261-016-0683-1
26. Hayakawa K, Tanikake M, Yoshida S, Urata Y, Yamamoto E, Morimoto T. Radiological diagnosis of large-bowel obstruction: neoplastic etiology. Emerg Radiol. 2013;20(1):69-76. http://dx.doi.org/10.1007/s10140-012-1088-2
27. Jaffe T, Thompson WM. Large-bowel obstruction in the adult: Classic radiographic and CT findings, etiology, and mimics. Radiology. 2015;275(3):651-63. http://dx.doi.org/10.1148/radiol.2015140916
28. Hussain ZH, Whitehead DA, Lacy BE. Fecal impaction. Curr Gastroenterol Rep. 2014;16(9). http://dx.doi.org/10.1007/s11894-014-0404-2
29. Saksonov M, Bachar GN, Morgenstern S, Zeina A-R, Vasserman M, Protnoy O, et al. Stercoral colitis: a lethal disease-computed tomographic findings and clinical characteristic. J Comput Assist Tomogr. 2014;38(5):721-6. http://dx.doi.org/10.1097/RCT.0000000000000117
30. Burrell HC, Baker DM, Wardrop P, Evans AJ. Significant plain film findings in sigmoid volvulus. Clin Radiol. 1994;49(5):317-9. http://dx.doi.org/10.1016/s0009-9260(05)81795-7
31. Javors BR, Baker SR, Miller JA. The northern exposure sign: A newly described finding insigmoid volvulus. AJR. 1999;173:571-4.
32. Lassandro G, Picchi SG, Romano F, Sica G, Lieto R, Bocchini G, et al. Intestinal pneumatosis: differential diagnosis. Abdom Radiol (NY). 2020. http://dx.doi.org/10.1007/s00261-020-02639-8.
33. Feczko PJ, Mezwa DG, Farah MC, White BD. Clinical significance of pneumatosis of the bowel wall. Radiographics. 1992;12(6):1069-78. http://dx.doi.org/10.1148/radiographics.12.6.1439012
34. Soyer P, Martin-Grivaud S, Boudiaf M, et al. Linear or bubbly: a pictorial review of CT features of intestinal pneumatosis in adults. J Radiol. 2008;89(12):1907-20.
35. Indiran V, Sivakumar V. Rigler sign. Abdom Radiol (NY). 2017;42(10):2588.http://dx.doi.org/10.1007/s00261-017-1149-9
36. Indiran V, Maduraimuthu P. Falciform ligament sign. Abdom Radiol (NY). 2017;42(4):1287-8. http://dx.doi.org/10.1007/s00261-016-0995-1
37. Marshall GB. The cupola sign. Radiology. 2006;241(2):623-4. http://dx.doi.org/10.1148/radiol.2412040700
38. Lin AC, Wu CC, Su CT. Classic signs of pneumoperitoneum on supine abdominal radiograph. Am J Emerg Med. 2006;24(5):642-3. http://dx.doi.org/10.1016/j.ajem.2005.12.023-Pubmedcitation
39. Sherman SC, Tran H. Pneumobilia: benign or life-threatening. Emerg Med. 2006;30:147-53.
40. Gosink BB. Intrahepatic gas: differential diagnosis. AJR Am J Roentgenol. 1981;137(4):763-7. http://dx.doi.org/10.2214/ajr.137.4.763
41. Chang L, Chang M, Chang HM, Chang AI, Chang F. Clinical and radiological diagnosis of gallstone ileus: a mini review. Emerg Radiol. 2018;25(2):189-96. http://dx.doi.org/10.1007/s10140-017-1568-5
42. Han SY, Tishler JM, Aldrete JS. Extraperitoneal gas: compartmental localization and identification of source. J Can Assoc Radiol. 1985;36(1):17-21.
43. Yacoub JH, Clark JA, Paal EE, Manning MA. Approach to cystic lesions in the abdomen and pelvis, with radiologic-pathologic correlation. Radiographics. 2021;41(5):1368-86. https://doi.org/10.1148/rg.2021200207
44. Gelfand DW. The liver: Plain film diagnosis. Semin Roentgenol. 1975;10(3):177-85. http://dx.doi.org/10.1016/0037-198x(75)90060-7
45. Sirakov V, Sirakova A, Izmirlieva S. New indirect X-ray symptoms of discrete hepatomegaly. Folia Med (Plovdiv). 1991;33(4):32-5.
46. Gunes SO, Akturk Y. Determination of splenomegaly by coronal oblique length on CT. Jpn J Radiol. 2018;36(2):142-50. http://dx.doi.org/10.1007/s11604-017-0704-1
47. Bundrick TJ, Cho SR, Brewer WH, Beachley MC. Ascites: comparison of plain film radiographs with ultrasonograms. Radiology. 1984;152(2):503-6. http://dx.doi.org/10.1148/radiology.152.2.6739823
48. Wixson D, Kazam E, Whalen JP. Displaced lateral surface of the liver (Hellmer's sign) secondary to an extraperitoneal fluid collection. AJR Am J Roentgenol. 1976;127(4):679-82. http://dx.doi.org/10.2214/ajr.127.4.679
49. Love L, Demos TC, Reynes CJ, Williams V, Shkolnik A, Gandhi V, et al. Visualization of the lateral edge of the liver in ascites. Radiology. 1977;122(3):619-22. http://dx.doi.org/10.1148/122.3.619
50. Zulfiqar M, Shetty A, Tsai R, Gagnon M-H, Balfe DM, Mellnick VM. Diagnostic approach to benign and malignant calcifications in the abdomen and pelvis. Radiographics. 2020;40(3):731-53. http://dx.doi.org/10.1148/rg.2020190152
51. Brown RC, Loening SA, Ehrhardt JC, Hawtrey CE. Cystine calculi are radiopaque. AJR Am J Roentgenol. 1980;135(3):565-7. http://dx.doi.org/10.2214/ajr.135.3.565
52. Fulgham PF, Assimos DG, Pearle MS, Preminger GM. Clinical effectiveness protocols for imaging in the management of ureteral calculous disease: AUA technology assessment. J Urol. 2013;189(4):1203-13. http://dx.doi.org/10.1016/j.juro.2012.10.031
53. Jones MW, Kashyap S, Ferguson T. Gallbladder Imaging. StatPearls Publishing; 2021
54. Kamat R, Gupta P, Rana S. Imaging in chronic pancreatitis: State of the art review. Indian J Radiol Imaging. 2019;29(02):201-10. http://dx.doi.org/10.4103/ijri.ijri_484_18
55. Mathew RP, Department of Radiology and Diagnostic Imaging, University of Alberta School of Medicine and Dentistry, Edmonton, Canada, Sam M, Alexander T, Patel V, Low G, et al. Abdominal and pelvic radiographs of medical devices and materials—Part 1: gastrointestinal and vascular devices and materials. Diagn Interv Radiol. 2020;26(2):101-10. http://dx.doi.org/10.5152/dir.2019.19390
56. Mathew RP, Department of Radiology and Diagnostic Imaging, University of Alberta School of Medicine and Dentistry, Edmonton, Canada, Sam M, Alexander T, Patel V, Low G, et al. Abdominal and pelvic radiographs of medical devices and materials-part 2: neurologic and genitourinary devices and materials. Diagn Interv Radiol. 2020;26(3):160-7. http://dx.doi.org/10.5152/dir.2019.19391.

Correspondencia

Felipe Aluja-Jaramillo
Hospital Universitario San Ignacio, Pontificia Universidad Javeriana
Carrera 7 # 40-62
Bogotá, Colombia
Correo electrónico: falujaj@husi.org.co

Recibido para evaluación: 20 de enero de 2022
Aceptado para publicación: 30 de abril de 2022